Paleoenvironmental and paleoclimatic conditions during the Eocene/Oligocene transition in the southern Hellenic Thrace Basin (Lemnos Island, North Aegean Sea)

SOFIA KOSTOPOULOU[1,✉], ANGELOS G. MARAVELIS[2],
CHRYSANTHOS BOTZIOLIS[1] and AVRAAM ZELILIDIS[1]

[1]Laboratory of Sedimentology, Department of Geology, University of Patras, 265 04 Rion, Greece; ✉kost.sofia@hotmail.com
[2]School of Geology, Aristotle University of Thessaloniki, 541 24 Thessaloniki, Greece

Abstract: The late Eocene–early Oligocene paleoenviromental and paleoclimatic conditions in the southern Hellenic Thrace Basin (Lemnos Island, Northeast Aegean Sea) have been determined, based on planktonic and benthic foraminiferal analyses. One hundred thirty-nine mudstone samples were collected from representative outcrops that cover the entire stratigraphic record. The samples correspond to submarine fan (Ifestia, Panagia and Kaspaka sections) and shallow-marine deposits (Kaminia section). The analyses of calcareous nannoplankton and planktonic foraminifera indicate that sedimentation took place during the late Eocene to early Oligocene (Priabonian–Rupelian). The ratio of planktonic to benthic foraminifera, the paleobathymetry and the qualitative analysis of foraminifera support a regional shallowing-upward trend. The presence of *Globobulimina* suggests that dysoxic conditions prevailed the late Eocene, while the presence of paragloborotaliids, globigerinids and chiloguembelinids in the studied succession could be indicative of a gradual cooling event since the late Eocene. The Eocene/Oligocene boundary is characterized by well-oxygenated bottom waters, and the abundance of *Catapsydrax unicavus* and *Paragloborotalia nana* suggests a strong cooling event during the early Oligocene (O1 biozone). This decrease in water temperature is most likely linked to the global cold Oi1 event. The early Oligocene is characterized by oxic bottom-water redox conditions that were intermittently interrupted by shorter periods of dysoxic conditions. The occurrence of *Bathysiphon* indicates the passage of turbidity currents. The recognition of *Chiloguembelina cubensis, P. nana* and *C. unicavus* suggests high productivity over the range of the water column, most likely correlated with mixing water during the cold event Oi2. This study decrypted the global paleoenvironmental and paleoclimatic changes that influenced the southern Hellenic Thrace Basin during the Eocene/Oligocene transition.

Keywords: planktonic foraminifera, Lemnos Island, southern Hellenic Thrace Basin, Eocene, Oligocene, Eocene–Oligocene boundary.

Introduction

The middle Eocene to early Oligocene is considered the transitional time from the warm climate of the Late Cretaceous to the cooler climate of the Neogene (e.g., Dall'Antonia et al. 2003). Several studies suggest that the temporal transition of Eocene–Oligocene has been influenced by: (a) climatic and oceanographic changes; and (b) reorganization of the tectonic plates (e.g., Berggren & Prothero 1992; Prothero 1994; Ozsvárt et al. 2016; Sancay & Batı 2020). The Oligocene period is characterized by large and sudden climate changes, paleogeographic changes, large variations in Antarctic ice thickness in the early Oligocene, and eustatic changes (e.g., Wade & Pälike 2004; Pälike et al. 2006). The formation of cold deep water in the Southern Ocean and/or the North Atlantic may have started since the early Oligocene (e.g., Kennett 1977; Miller et al. 1991, 2005; Zachos et al. 2001; Lawver & Gahagan 2003), but this hypothesis is still under study (e.g., Barker & Thomas 2004; Scher & Martin 2004; Via & Thomas 2006; Thomas 2007; Thomas et al. 2008). These climatic variations occur in orbital/circular patterns (Wade & Pälike 2004; Coxall et al. 2005; Pälike et al. 2006), with some of the most extreme cold events occurring during low obliquity.

The identification of the global paleoenvironmental development throughout the Eocene/Oligocene transition requires the integration of data from different regions, with dissimilar bathymetry. Microfossils are thought as a useful tool for such paleoenvironmental representations. Planktonic foraminifera are very important biostratigraphic and paleoceanographic indicators, because of their morphological characteristics, properties, and geochemical composition (e.g., Berggren et al. 1995; Wade et al. 2011). Planktonic foraminifera may provide information about their living environment because they are directly affected by changes in temperature, salinity, and primary productivity (e.g., Bernhard & Sen Gupta 1999). Benthic foraminifera are also very important paleoceanographic indicators because of their high diversity and abundance in marine sediments and their sensitivity to environmental changes and disturbances. The composition of benthic foraminifera assemblages and the species morphology add constraints about the sediment water interface, the water column depth, and the sea-water chemistry. They are also considered as good

indicators of oxygenation levels, concentration of organic matter in bottom waters, and rate of circulation of water masses (e.g., Douglas & Woodruff 1981; Corliss et al. 1986; Hermelin & Shimmield 1995; Schmiedl et al. 1998). Benthic foraminifera are also good paleodepth indicators (e.g., Natland 1933; Bandy 1960).

Studies of Oligocene benthic foraminifera from the Eastern Mediterranean and surrounding regions are rare, despite the regional paleogeographical importance (Barbieri 1992; Ozsvárt et al. 2016; Nyerges et al. 2020). The detailed bio-stratigraphic and paleoenvironmental analysis of the upper Eocene to lower Oligocene sedimentary succession in the southern Hellenic Thrace Basin (referred to herein southern HTB, Lemnos Island) reveals the relationship between the eco-sedimentary agents and the paleoenvironmental dynamics. This research adds to the recently published work of Kostopoulou et al. (2018) that examined the paleoenvironment and the paleoceanography of the region, using detailed micropaleontological (benthic and planktonic foraminifera assemblages) analysis. This research elaborates benthic and planktonic foraminiferal analyses to study the reflection of global paleoclimatic signals in low to mid latitude settings, such as the southern HTB.

## Regional geology and basin fill history

The Hellenides are an arcuate orogen, developed above the subducting Hellenic plate. From north to south, the Aegean region encompasses several geotectonic zones including the: (a) Rhodope and Serbo–Macedonian massif (RSM); (b) Circum-Rhodope Belt (CRB); (c) Pelagonian zone; (d) Vardar–İzmir–Ankara oceans; and (e) Pindos ocean (e.g., Robertson et al. 1991; van Hinsbergen et al. 2005). The HTB is a large sedimentary basin that is interpreted as a two-sided forearc basin during the Eocene–Oligocene. In the Aegean region, the forearc trinity is composed of the southern-located accretionary prism (Pindic Cordillera), the HTB forearc basin (HTB) and the northern-located Rhodopian magmatic arc (Maravelis et al. 2007; Tranos et al. 2009; Maravelis & Zelilidis 2013). The northern HTB was influenced by the Rhodopian magmatic arc. The basin is filled with sediment that comes from the north and displays a continental arc signature (Maravelis & Zelilidis 2010; d'Atri et al. 2012; Maravelis et al. 2016). The Rhodopian magmatic arc developed as a result of the subduction of the Vardar–İzmir–Ankara oceans and parts of the Pelagonian–Lycian Block. Subduction processes initiated in southern Bulgaria at ~90–75 Ma (von Quadt et al. 2005). Above the southern edge of the Pelagonian–Lycian Block, the HTB was formed by Eocene (~56–50 Ma) (Ring et al. 2010). The impact of the growing accretionary prism is recorded in the basin fill history of the southern HTB (Maravelis & Zelilidis 2010). This accretionary prism delivered sediment of intermediate to mafic composition (Maravelis & Zelilidis 2010) to the north-northeast (Maravelis et al. 2007). The southern HTB records an upward-shoaling sedi-

mentary succession, with submarine fans overlain by shallow-marine deposits between the late Eocene to Oligocene. Given the low to moderate eustatic sea-level changes during this time period (Miller et al. 2011), it has been suggested that this shoaling-upward trend is the result of tectonically-driven uplift and compression (Maravelis et al. 2007, 2015), and it is further supported by the back stripping analysis (Maravelis et al. 2016).

In the southern HTB, the submarine fan system (~300 m thick) is sand-rich and consists of both outer and inner fan deposits (Maravelis et al. 2007). The outer fan is thicker (~150–200 m thick), lowered positioned and consists of lobe, inter-lobe, lobe-fringe, and fan-fringe deposits (Fig. 1). The overlying inner fan is sub-divided into a lower, sand-dominated part (~50 m) and an upper conglomeratic part (~50 m). Both sub-divisions include channel-fill and levee deposits. The degree of amalgamation is greater in the inner than the outer fan, as a result of the greater erosional ability of thick, high-speed, and strongly turbulent flows (Maravelis & Zelilidis 2011). The bedding in the outer fan deposits is simple and laterally continuous. In contrast, inner fan deposits display a complicated bedding pattern with temporal and spatial random distribution of channelized deposits and higher degree of erosion. The southern HTB is filled principally with submarine fan deposits and gradually shoals upwards into slope (~20 m thick) and shallow-marine deposits (~90 m thick). The proposed sequence stratigraphic scenario (Maravelis & Zelilidis 2011; Maravelis et al. 2015) indicates that the succession is dominated by regressive deposits and displays progradation of depositional environments into shallower waters (Fig. 2). The submarine fans are interpreted as forced regressive, deposited during a period of relative sea level fall. The overlying slope deposits accumulated during subsequent sea level rise. The lower part of the slope deposits was accumulated during lowstand normal regression whereas the upper part was accumulated during transgression. Further up-sequence, the shallow marine deposits accumulated during a highstand normal regression.

Material and methods

The micropaleontological analysis was performed by collecting mudstone samples from the different environments of deposition (submarine fans, slope and shallow-marine). The sequence stratigraphic framework of Maravelis & Zelilidis (2011) and Maravelis et al. (2016) adds tight lithostratigraphic constraints and was utilized to secure that the samples cover the entire succession and are collected from the correct stratigraphic level. Therefore, four stratigraphic sections were selected, and 139 samples were analyzed. The Ifestia section is ~95 m thick (38 samples with resolution ~2.5–3 m) and is sub-divided into three parts. The lower part is ~50 m thick and is represented by distal submarine fan deposits (lobes). The middle part is ~35 m thick and corresponds to proximal submarine fan deposits (channel-fills and overbanks). The upper
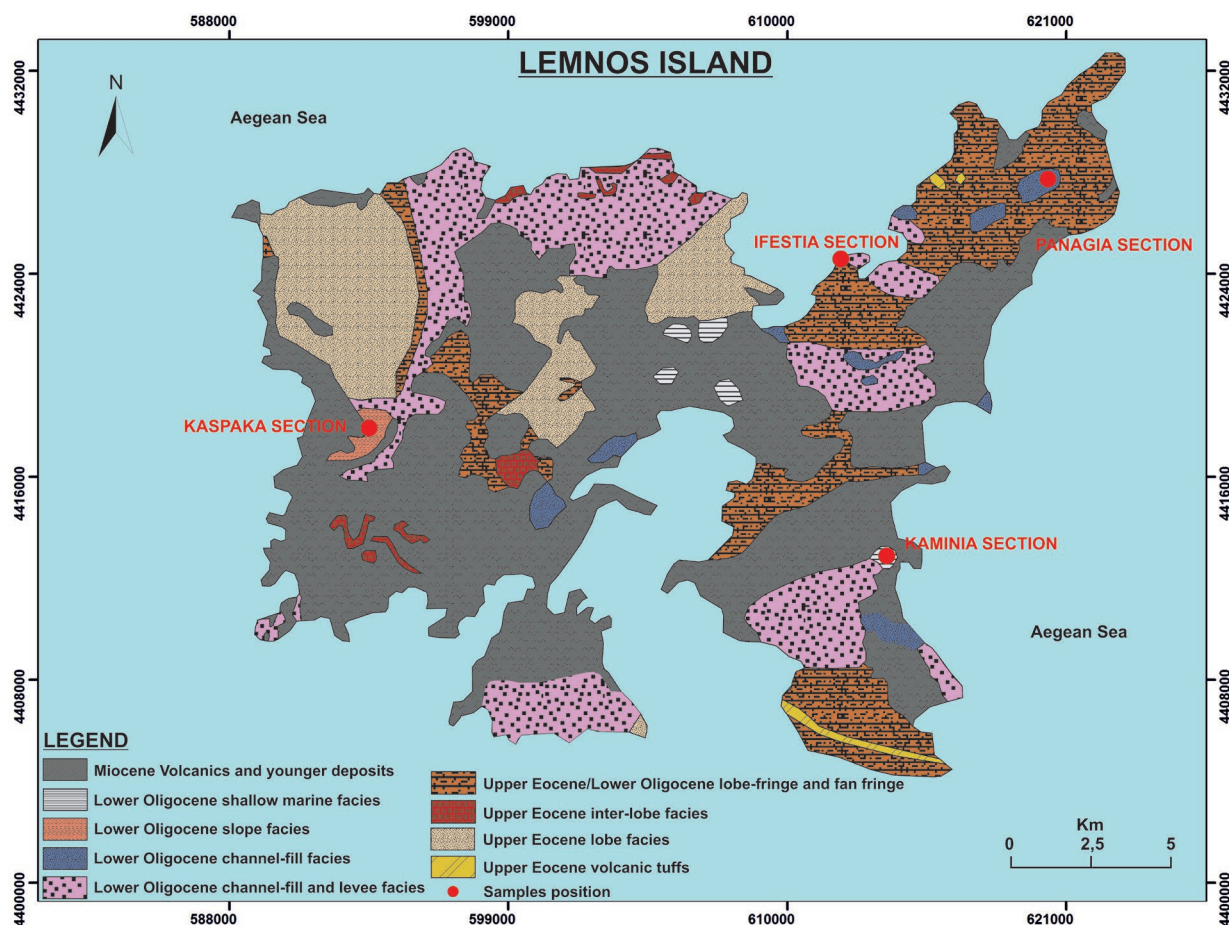
Fig. 1. Detailed geological map of the southern HTB (Lemnos) illustrating the spatial distribution of the studied deposits (modified from Maravelis & Zelilidis 2011). Note the different depositional environments and sub-environments. Black dots correspond to the studied sections. Paleocurrent analysis is from Maravelis et al. (2007, 2015).

part is ~10 m thick and is represented by coarser-grained, proximal submarine fan deposits (conglomeratic channel-fills and overbanks). The Panagia section is ~30 m thick (36 samples with resolution ~0.5–1.5 m) and is composed of two parts. The lower part is ~10 m thick and is composed of proximal submarine fan deposits (channel-fills and overbanks), while the upper part is ~20 m thick and consists of coarser-grained, proximal submarine fan deposits (conglomeratic channel-fills and overbanks). The Kaspakas section is ~50 m thick (20 samples with resolution ~2.5–3 m) and is divided into two parts. The lower part is ~10 m thick and is represented byproximal submarine fan deposits(channel-fills and overbanks). The upper part is ~40 m thick and is composed of continental slope deposits. The Kaminia section is ~100 m thick (45 samples with resolution ~1–2.5 m) and is represented by shallow-marine deposits. The detailed sedimentological analysis of the studied deposits is presented in Maravelis et al. (2007) and Kostopoulou et al. (2018).

The studied sediments accumulated in Lemnos Island during the late Eocene to early Oligocene. The detailed calcareous nannofossils and planktonic foraminifera analysis confirm the biostratigraphic interval E14-O4 (Wade et al. 2011;

planktonic foraminifera zonation) and CNE18-CNO4 (Agnini et al. 2014; calcareous nannofossils zonation) for the study area (Kostopoulou et al. 2018).

Foraminifera analysis

The samples were collected from the land sections (Ifestia section, Panagia section, Kaspakas section and Kaminia section) according to the regional sequence stratigraphic framework. One hundred thirty-nine sediment samples (150–200 g dry weight each) were prepared for foraminiferal analysis using standard techniques. Each sample(150–200 g dry sediment) was decomposed using hydrogen peroxide (H_2O_2) and was subsequently ultrasonicated to enhance decomposition. Some samples were soaked in acetic acid (80 % CH_3COOH and 20 % H_2O) for maximum 2 h, because of the strong cementation. The samples were then washed through a 63-µm sieve, and were dried at 50 °C. The samples exhibit high degree of lithification and thus, multiple treatments were required to achieve decomposition. An Otto microsplitter was used to split the dry material. At least 300 specimens were
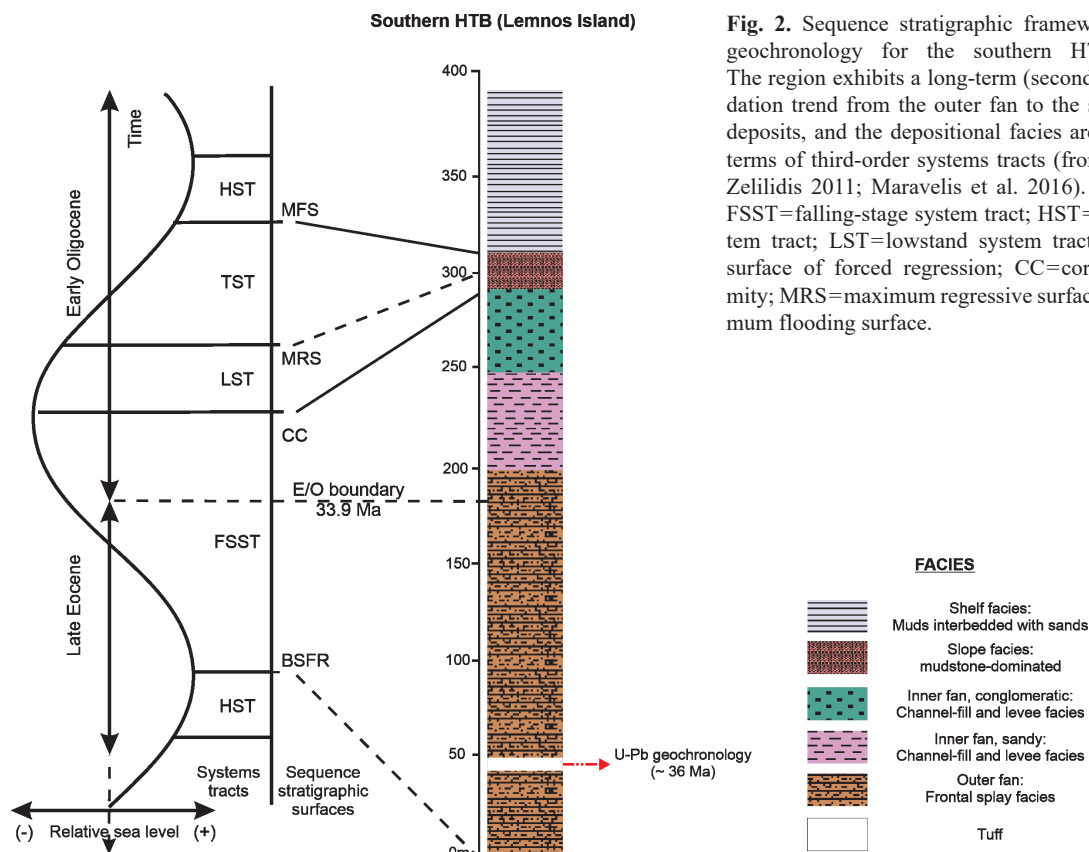
Fig. 2. Sequence stratigraphic framework and U–Pb geochronology for the southern HTB (Lemnos). The region exhibits a long-term (second order) progradation trend from the outer fan to the shallow-marine deposits, and the depositional facies are interpreted in terms of third-order systems tracts (from Maravelis & Zelilidis 2011; Maravelis et al. 2016). Abbreviations: FSST=falling-stage system tract; HST=highstand system tract; LST=lowstand system tract; BSFR=basal surface of forced regression; CC=corelative conformity; MRS=maximum regressive surface; MFS=maximum flooding surface.

collected and identified under a Leica S4E stereoscope, at 80× magnification. The systematic taxonomy of Wade et al. (2018) was elaborated for planktonic foraminifera. The genus or/and family of benthic foraminifera was utilized to calculate the following indices:

- Planktonic/benthic ratio, using the formula (P/B %)=N_p ×100/(N_p+N_b). Nb corresponds to the number of benthic foraminifera and N_p to the number of planktonic foraminifera (van der Zwaan et al. 1990, 1999). The environmental divisions of Murray (1991) were used for data interpretations: (a) inner shelf (<20 %), (b) middle shelf (20–50 %), (c) outer shelf (50–70 %) and (d) upper bathyal zone (>70 %).
- Calcareous/agglutinated ratio, using the formula (C/A %)= N_c×100/(N_c+N_a). N_c corresponds to the number of calcareous foraminifera and Na to the number of agglutinated foraminifera. This formula was used merely for benthic foraminifera, as suggested by Ortiz et al. (2011).
- Infaunal/epifaunal ratio, using the formula (In/Ep %)=N_{in} ×100/(N_{in}+N_{ep}).Nin corresponds to the number of infaunal calcareous benthic foraminifera and N_{ep} to the number of epifaunal calcareous benthic foraminifera. This formula was used as an index of bottom water oxygenation (Ortiz et al. 2011).

The grouping of infaunal and epifaunal forms was based on studies of the microenvironments of living benthic foraminifera, such as Corliss (1985), Corliss & Chen (1988), Jorissen et al. (1995), den Dulk et al. (2000), Thomas et al. (2000), Alegret et al. (2003) and Murray (2006). Infaunal

forms include representatives of the taxa *Bolivina, Globobulimina, Chilostomella, Bulimina, Nonionella, Melonis, Pullenia, Nonion, Uvigerina,* nodosarids*, Globocassidulina* and *Cassidulina*, while epifaunal forms include both shelf (*Elphidium, Rosalina, Ammonia*, miliolids, *Ammodiscus* and *Discorbis*) and deep-water dwellers (*Cibicides/ Cibicidoides, Lenticulina, Siphonina* and *Gyroidinoides*).

- Benthic Foraminiferal Oxygen Index (Kaiho 1994, 1999), using the formula BFOI=a/(a+n)×100 (a is the number of oxic species and n is the number of dysoxic species). When a=0 and n+s>0 (s is the number of suboxic species), the BFOI is calculated using the formula [(s/(s+n))−1]×50. According to Kaiho (1994) oxic indicators include representatives of the taxa *Globocassidulina, Siphonina, Cibicides/Cibicidoides, Elphidium, Rosalina, Ammonia*, miliolids, *Ammodiscus* and *Discorbis*, suboxic indicators include representatives of *Bulimina, Nonionella, Melonis, Pullenia, Nonion, Uvigerina*, nodosarids, *Cassidulina, Gyroidinoides* and *Lenticulina* while dysoxic indicators include representatives of *Bolivina, Globobulimina* and *Chilostomella*.

According to Kaiho (1994) four different oxygen conditions are recognized: (1) high oxygen conditions (values 50–100 %, presence of dysoxic, suboxic and high ratios of oxic indicators); (2) low oxygen conditions (values 0–50 %, presence of dysoxic, suboxic and low ratios of oxic idicators); (3) suboxic conditions (values −40–0 %, presence of dysoxic and high ratios of suboxic indicators); (4) dysoxic conditions (values −50 to −40 %, presence of dysoxic and

low ratios or barren of suboxic indicators); and (5) anoxic conditions (values −55 %, absence of calcareous benthic foraminifera).

Results

Benthic foraminifera

The benthic foraminifera assemblages are composed of *Lenticulina, Cibicides, Rosalina, Nonion, Bolivina, Bulimina, Nonionella, Globocassidulina, Bathysiphon, Elphidium, Gyrodinoides, Melonis, Pullenia, Ammodiscus, Globobulimina, Uvigerina*, as well as individuals of nodosariidae, miliolids and agglutinants. On this study, benthic foraminifera grouped in infaunal, epifaunal (deep water and shelf dwellers), oxic, suboxic and dysoxic indicators.

Ifestia section (upper Eocene–lower Oligocene)

The infaunal assemblages present a grade range from 5 % to 78.9 %. The highest abundance (78.9 %) is identified at 23.1 m (sample L65; upper Eocene) while the lowest (5 %) is observed at 70.06 m (sample L9; lower Oligocene). Shelf dwellers show a similar pattern, with the lowest value of 2.9 % to be identified at 58.42 m (sample L15; lower Oligocene) and the highest value of 82.4 % at 54.54 m (sample L17; lower Oligocene). The deep-water indicators present sporadic occurrences reaching up to 44.4 % at sample L90 (upper Eocene), 15.8 % at sample L65 (upper Eocene) and 62.5 % at sample L50 (EOB). The highest occurrence (up to 85 %) is observed at the upper part of the section (sample L9; lower Oligocene). The oxic indicators range from 4 % (sample L31; lower Oligocene) to 82.4 % (sample L17; lower Oligocene) while the same pattern is identified at suboxic indicators (up to 66.7 % at 58.42 m and up to 2.7 % at 85.58 m). In contrast, dysoxic indicators assemblages show the highest value (73.7 %) at the lower part of the section (L65; upper Eocene). The upper part of the section (lower Oligocene) characterized by a maximum of 25 % at sample L13 and a minimum of 4.3 % at samples L15 and L19 (Fig. 3a).

The P/B also shows high values in this section, with a maximum of 97 % at 33 m (sample L50; EOB). High values are identified at 6.6 m (L90; 96.4 %) and at 23.1 m (L65; 57.8 %) of late Eocene time interval. A similar pattern is shown in the diagram of the C/A % ratio that reaches up to 100 % mainly in the lower part of the section (L90, L65 and L50). Throughout the section, fluctuations in the C/A % ratios are observed, with the most intense being located at the upper part. These fluctuations display a maximum of 100 % at samples L17 and L13 and a minimum of 15 % at sample L9 in the early Oligocene time interval. The In/Ep % ratio ranges from 12.5 % (sample L17) to 100 % (sample L7), while of interest is the abruptly decrease of that ratio in the L5 sample. BFOI index fluctuates in Ifestia section, with generally high values in samples L90 (75), L50 (66.7), L9 (100), L5 (100) and L3 (100), and low

values in samples L65 (6.7), L31 (25) and L7 (0) (Fig. 3b). Finally, agglutinants and especially *Bathysiphon* is observed at samples L28 and L26 (lower Oligocene) with values of 5.9 % and 3.7 %, respectively. Agglutinants fluctuate in the upper part of the section and reach maximum abundance at 70.06 m (sample L9; lower Oligocene) (Fig. 3a).

Panagia section (lower Oligocene)

The infaunal indicators fluctuate in the Panagia section. The lower values (3.7 %) are identified at 11.9 m (sample R17) and the highest (up to 61.8 %) at 20.9 m (sample R35). The shelf dwellers display fewer and sporadic occurrences. The maximum value (23.5 %) is observed at 11.9 m (sample R17), while the minimum (1.3 %) at 10.4 m (sample R14). The top of Panagia section lacks of shelf dwellers, in contrast to the deep-water dwellers that fluctuate with higher percentages. The highest abundances are observed in the middle and upper part of the section. They range from 78.6 % (sample R30; 18.4 m) to 23.5 % (sample R35; 20.9 m).The higher values of oxic indicators are identified in the middle to upper part of the section, where they reach up to 76.8 % at 18.4 m (sample R30). Suboxic indicators display a similar pattern, with stronger fluctuations at the base and the top of the section. The maximum values are observed in samples R0 (69.2 %), R7 (66.7 %) and R45 (78.3 %). The dysoxic indicators generally occur at lower values. The highest abundances of 41.7 %, 55.9 % and 40 % are observed at 0.45 m (sample R0.8; base of section), 20.9 m (sample R35; top of section) and 23.9 m (sample R41; top of section), respectively (Fig. 4a).

The P/B fluctuates and possesses the highest abundance (up to 98.7 %) at 7.2 m (sample R7). The top of the section displays the lower values of 58.3 % and 20.7 % (samples R41, 23.9 m and R45, 25.9 m respectively). The C/A % ratio show a similar pattern with stronger fluctuations. Several samples are presenting C/A % ratio of 100 % because of the absence of agglutinants. The In/Ep % ratio fluctuates in the section and exhibits the highest values in sample R0.8 (54.5 %), R0 (53.8 %) and R41 (up to 100 %). The fluctuations are also common feature of the BFOI index, which ranges from 100 (samples R0.2, R14, R17 and R45) to −50 (sample R41) (Fig. 4b). The benthic foraminifera *Bathysiphon* and agglutinants are observed almost in the entire section. The highest abundance (60 %) of *Bathysiphon* is identified at 23.9 m (sample R41), while the maximum value (42 %) of agglutinants is observed at the middle part of the section (11.9 m; sample R17) (Fig. 4a).

Kaspakas section (lower Oligocene)

The micropaleontological analysis that performed in the Kaspakas section did not reveal any benthic foraminifera, most likely because of the hostile conditions of preservation. Only calcareous nannofossils were observed at that section (Kostopoulou et al. 2018).
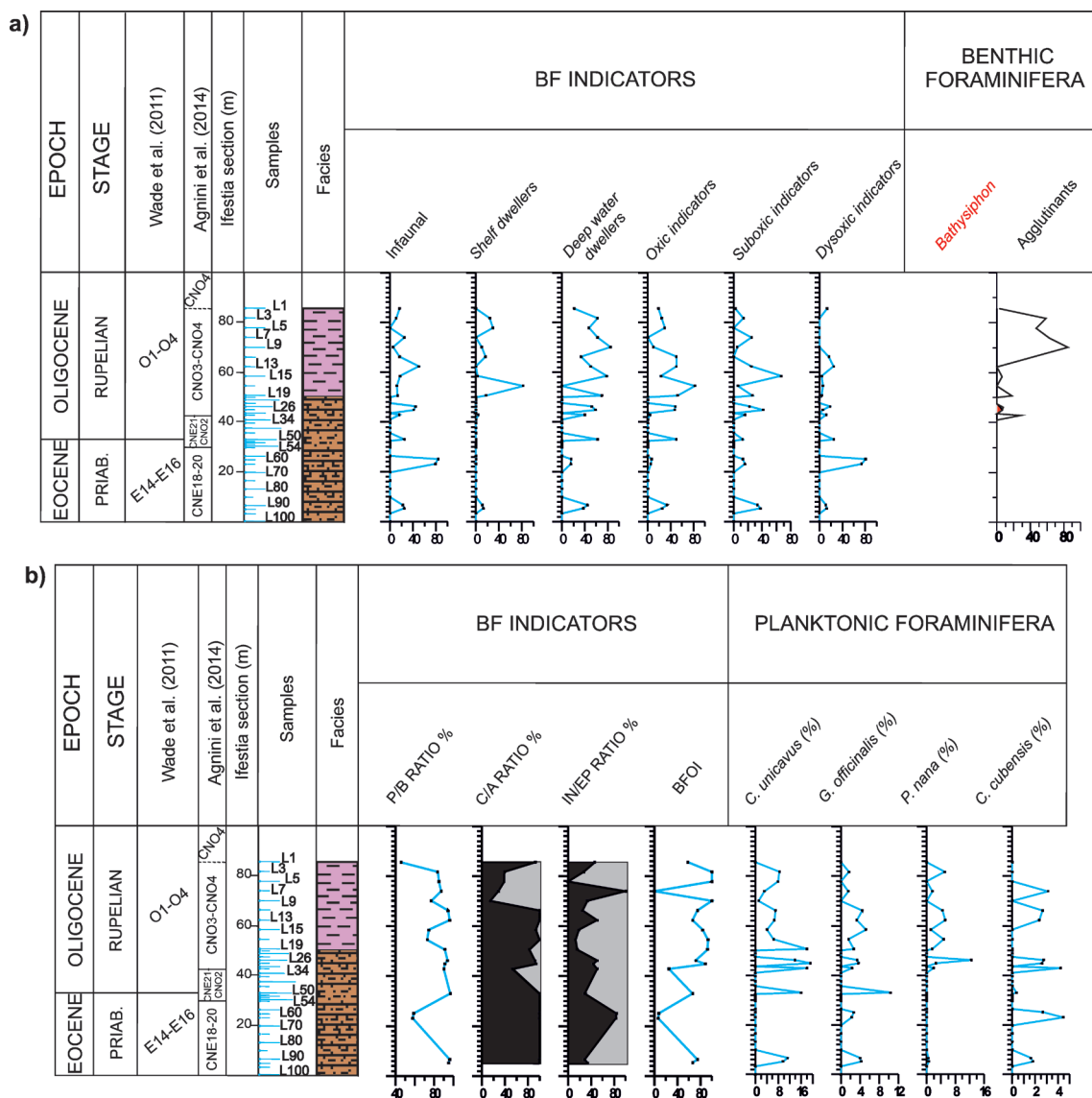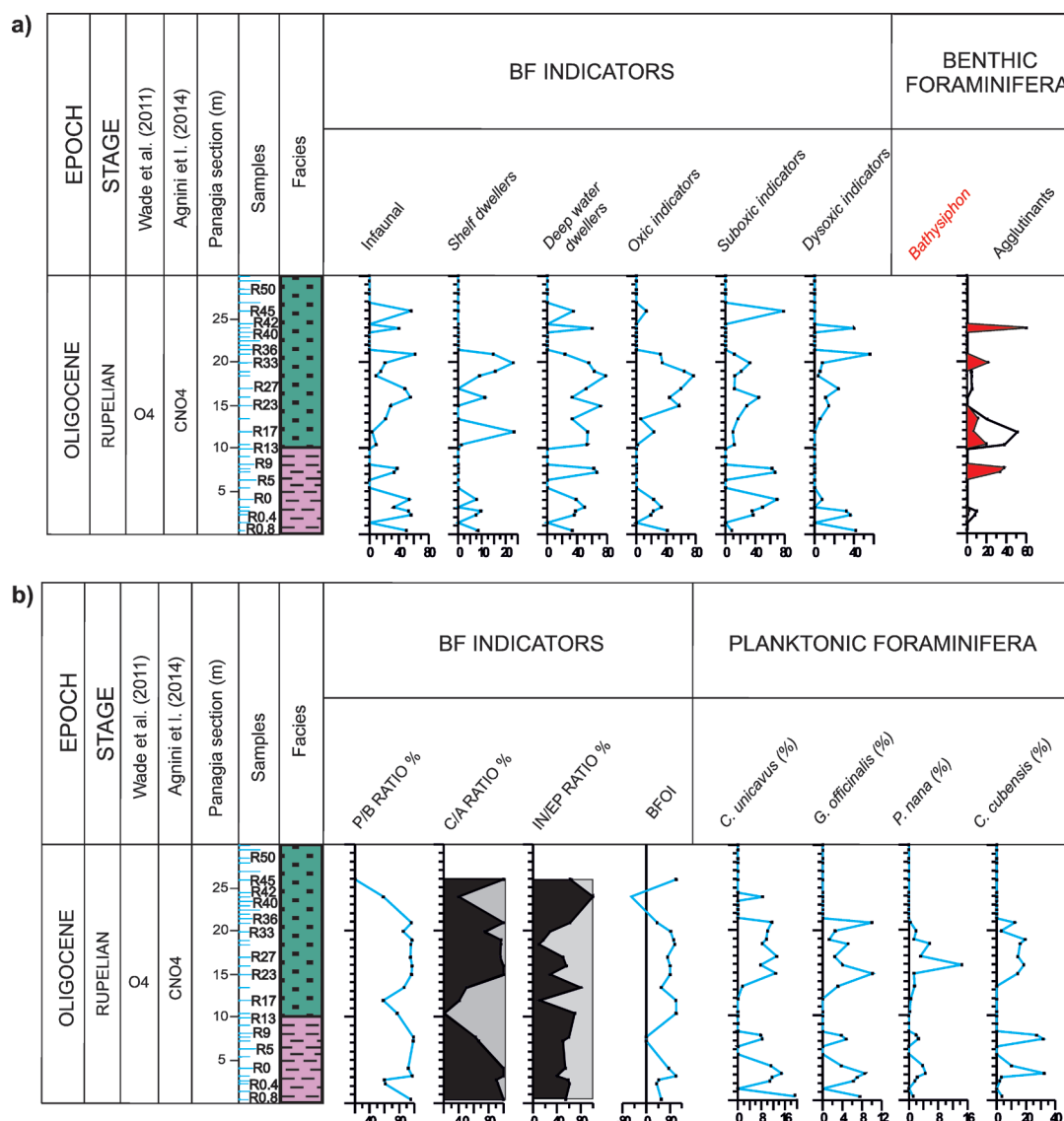
Fig. 3. a — Relative abundances (%) of benthic foraminifera in association with sedimentary facies as specified in Ifestia section; **b** — Distribution of benthic foraminifera indicators, the relative abundances of benthic foraminifera and relative abundances (%) of selected planktonic foraminifera in association with sedimentary facies as specified in Ifestia section. Lobe facies is the lower 50 m layers, while channel-fill facies is the upper 35 m layers.

Kaminia section (lower Oligocene)

The abundance of infaunal indicators fluctuates in this section. In the lower part, it ranges between 46.2 % (sample D40, 25.6 m) and 23.9 % (sample D28). In the middle part, it fluctuates between 75 % (sample D59) and 18.8 % (sample D49). In the upper part, it ranges between 40.2 % (sample D68) and 25.4 % (sample D17). Shelf dwellers occur at low levels, with a maximum of 4.7 % at 93.44 m (sample D4). In contrast, deep-water dwellers occur at high values in most of the samples, reaching a maximum value of 74.6 % (sample D17). Oxic indicators display high values in this section and the highest abundance (76.9 %) is identified in the sample D18 (90.88 m). The suboxic and dysoxic indicators display the same pattern, but with lower abundances (maximum suboxic

indicators: 31.3 % in sample D59; maximum dysoxic indicators: 44.4 % in sample D51) (Fig. 5a).

The P/B exhibits very high values. An almost stabilized index is identified with a value not exceeding 89 % (sample D28). A low increase (up to 93.3 %) is detected in sample D49. Then the ratio is stabilized in lower values in the upper part of the section. These values range at ~60 %. The C/A % ratio occur in 100 % across the section, as no agglutinants are observed. The In/Ep % ratio is also marked by fluctuations. The lower part of the section is characterized by low ratios that do not exceed 32.4 % (sample D21). At this lower part of the section, an abrupt degrease (23.1 %) occurs (37.12 m, sample D49). A maximum In/Ep % ratio of 75 % is identified at 49.92 m (sample D59), and from this stratigraphic level, the In/Ep % ratio gradually decreases upwards. The BFOI index

Fig. 4. a — Relative abundances (%) of benthic foraminifera in association with sedimentary facies as specified in Panagia section; **b** — Distribution of benthic foraminifera indicators, the relative abundances of benthic foraminifera and relative abundances (%) of selected planktonic foraminifera in association with sedimentary facies as specified in Panagia section. Channel-fill facies is the lower 10 m layers, while channel-fill facies with conglomerate is the upper 20 m layers.

displays a value of 80.8 (sample D19), at the basal part of the section. It exhibits small-scale fluctuations up to sample D49, where it reaches a value of 100. Up section, the BFOI index decreases sharply to 42.9 (samples D51 and D54) and then increases up to the top of the section, with values ranging from 80 (sample D69) to 83.3 (sample D4), while that index occurs in zero due to the absence of foraminifera (Fig. 5b).

Planktonic foraminifera

Several planktonic foraminifera have been identified in Lemnos Island, including *C. unicavus, G. officinalis, P. nana* and *C. cubensis*. These species are employed to unravel the paleoenvironmental and paleoclimatic conditions of the study region. It is worth noticing that the planktonic foraminifera

provide a clear reduction in the size of the test. The small size of the test in the context of dwarfing entails stress-induced conditions (Ozdínová & Soták 2014).

Ifestia section (upper Eocene–lower Oligocene)

C. unicavus occurs with a concentration that reaches a value of 11.2 % in sample L90 (6.6 m; upper Eocene) and then, in sample L50 (EOB), the concentration reaches a value of 16 %. The highest abundance (19.3 %) occurs at 44.88 m (sample L28; lower Oligocene). The upper part of the section is characterized by fluctuations of the species that range, but in much lower percentages. They display a minimum value of 1.1 % in sample L9 (70.06 m) and a maximum value of 8.4 % in sample L3. The first occurrence of *G. officinalis* occurs at
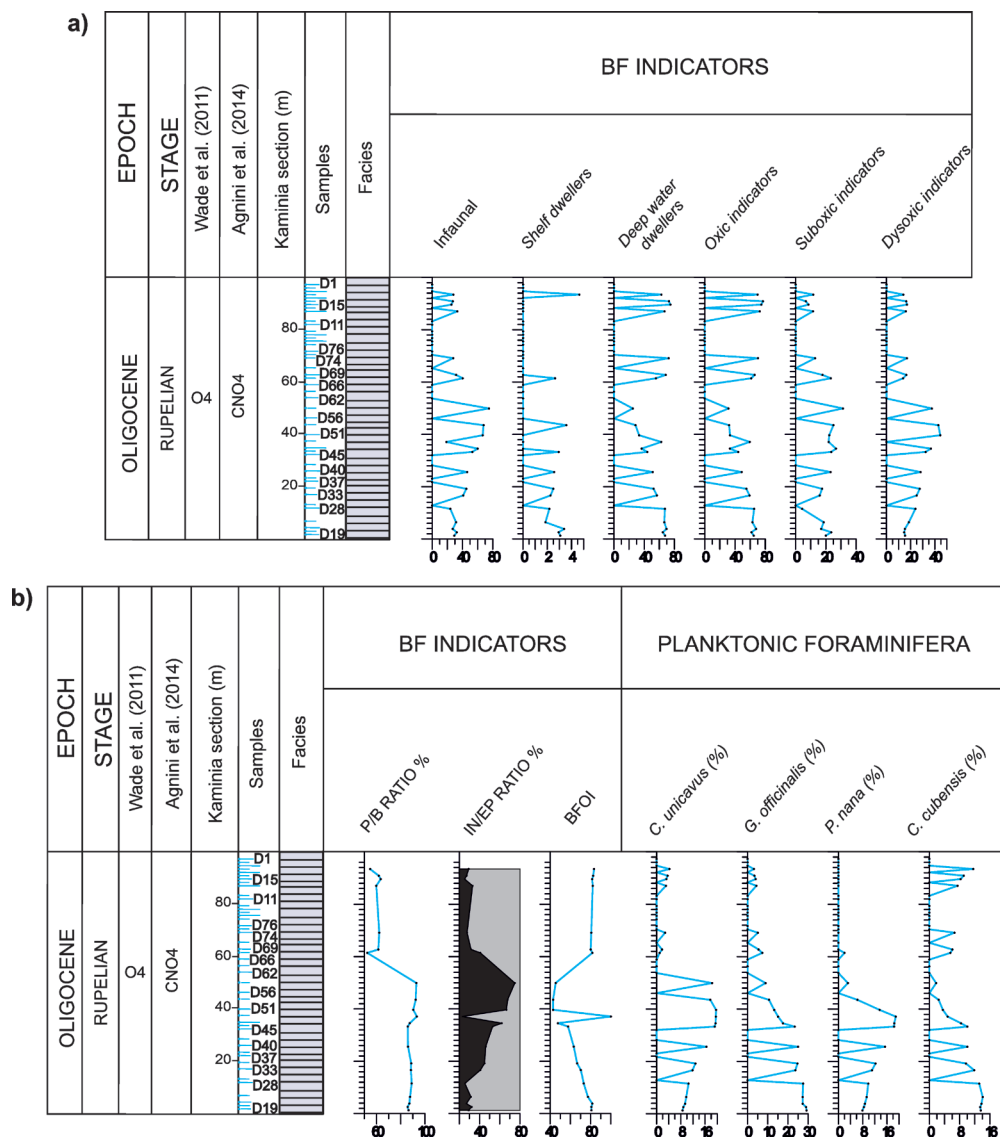
Fig. 5. a — Relative abundances (%) of benthic foraminifera in association with sedimentary facies as specified in Kaminia section; **b** — Distribution of benthic foraminifera indicators, the relative abundances of benthic foraminifera and relative abundances (%) of selected planktonic foraminifera in association with sedimentary facies as specified in Kaminia section (shelf facies).

the level of 6.6 m (sample L90; up to 4 %) but is absent until the level of 23.1 m (sample L65; 2.2 %). Up-section, this species increases and reaches a maximum value of 10.4 % in sample L50 (EOB). The first appearance of *P. nana* is identified at the base of the section (6.6 m; sample L90; up to 0.4 %). The highest abundance of *P. nana* (12.5 %) is identified at the level of 46.2 m (sample L26). The abundance of *C. cubensis* ranges at generally lower rates, and it is firstly observed with values up to 1.6 % at the level of 6.6 m (sample L90; upper Eocene). Up-section, the abundance of this species increases to reach a maximum of 4.4 % at the level of 23.1 m (sample L65; upper Eocene). However, at the level of 33 m (sample L50; EOB) is almost absent (0.4 %). Further up-section, the abundance of *C. cubensis* increases and reaches values up to 4.2 % at the level of 42.9 m (sample L31; lower Oligocene). It is then decreased at the level of 62.3 m (sample L13; 2.3 %),

before the final increase (up to 3.1 %) at the level of 73.94 m (sample L7; lower Oligocene) (Fig. 3b).

Panagia section (lower Oligocene)

C. unicavus firstly occurs at the level of 0.45 m (sample R0.8), with a concentration of 19.4 %. This section displays several fluctuations and includes five maxima at the levels of 2.25 m (sample R0.4; 10.8 %), 3.15 m (sample R0.2; 14.8 %), 4.05 m (sample R0; 11.2 %), 14.9 m (sample R23; 12.8 %) and 20.9 m (sample R35; 11.6 %). *G. officinalis* documents a similar pattern throughout the section whereas the samples R23 and R35 display the highest abundances (10.1 % and 10 % respectively). *P. nana* is also present, but with relatively low to zero abundances. The sample R25 exhibits the highest concentration of *P. nana* (14.4 %). Finally, *C. cubensis* is pre-

sent at high concentrations, especially at the lower part of the section. *C. cubensis* has maximum abundances (32.3 % and 31.7 %) at the levels of 3.15 and 7.2 m (sample R0.2 and R7 respectively). The abundance of *C. cubensis* fluctuates towards the upper part of the section, where it becomes absent (Fig. 4b).

Kaspakas section (lower Oligocene)

The micropaleontological analysis that conducted in Kaspakas section did not reveal any planktonic foraminifera, most likely because of the conditions of preservation. Only calcareous nannofossils were observed (Kostopoulou et al. 2018).

Kaminia section (lower Oligocene)

C. unicavus appears at the lower part of the section and has an abundance of 8.6 % (sample D19). This abundance gradually increases up-section and reach a value of 19.6 % at the level of 39.68 m (sample D51). Another maximum, with a value of 18.3 % occurs the level of 49.92 m. This is followed by levels of low to zero values until the following maxima (up to 3.1 % and 4.2 %) at the levels of 87.04 m (sample D15) and 93.44 m (sample D4) respectively. The abundance of *G. officinalis* reaches values up to 29.2 % (sample D19), gradually decreases at the level of 16.64 m (sample D33, 23.7 %), and increases again at the level of 25.6 m (sample D40; 25 %). The abundance of *G. officinalis* is low in the upper part of the section. The first appearance of *P. nana* is recognized in sample D19 (abundance up to 7.9 %) and its concentration gradually increases, reaching a value of 18.9 % at the level of 37.12 m (sample D49). The abundance of *P. nana* is low in the upper part of the section. Finally, *C. cubensis* is relatively abundant (up to 13.6 %) at the base of Kaminia section (sample D19). The highest abundance is identified at the level of 6.4 m (sample D24; 14.1 %) and then it gradually decreases at the level of 19.2 m (sample D35; 9.7 %), fluctuating up to sample D4 (11.6 %) (Fig. 5b).

Discussion

Paleobathymetry

Paleobathymetric analysis adds tighter constraints to the reconstruction of depositional environments and can enhance geological and paleoceanographic interpretations (e.g., Zivkovic & Babic 2003). The micropaleontological assemblages in marine depositional environments have been widely employed to estimate the paleobathymetry and the P/B is an important indicator for the paleodepth determination (e.g., van der Zwaan et al. 1990, 1999; Alegret et al. 2008; Fenero et al. 2012).

Several studies have confirmed the positive correlation between the percentage of planktonic foraminifera and the increasing water depth of deep-sea basins (e.g., Gibson 1988; van der Zwaan et al. 1990; Nigam & Henriques 1992).

However, local conditions (e.g., water circulation, stratification of the water column, upwelling and distribution of water masses) can greatly affect the production rate of shells in both planktonic and benthic foraminifera and therefore the P/B ratio (e.g., Gibson 1988; van der Zwaan et al. 1990; Nigam & Henriques 1992; Ozdínová & Soták 2014). On the other hand, this positive correlation reflects the reduction of organic matter that is transported from surface to bottom waters, with increasing water depth (e.g., Berger & Diester-Haass 1988). For the paleobathymetry, water depth (D, in meters) is illustrated by the equation: $D = e[3.58718 + (0.03534 * \%P)]$ that was proposed by van der Zwaan et al. (1990). In the above equation, the infaunal benthic foraminifera are excluded because they do not directly depend on the supply of organic matter from the overlying water layers (van der Zwaan et al. 1990), and their incorporation reduces data scatter from different regions.

The study area covers the late Eocene/early Oligocene time interval (Kostopoulou et al. 2018). In that time interval (Figs. 3–5), the benthic foraminifera are characterized by the significant presence of calcareous forms that live on the shelf and in the bathyal zone (e.g., *Bolivina, Bulimina, Melonis, Globobulimina, Globocassidulina, Lenticulina, Cibicides/ Cibicidoides*, nodosarids). Another feature is the occurrence of *Bathysiphon* that is agglutinant benthic foraminifera and lives in the bathyal zone (Corliss 1985; Corliss & Chen 1988; Jorissen et al. 1995; den Dulk et al. 2000; Thomas et al. 2000; Alegret et al. 2003; Murray 2006). However, several samples (mainly from the Ifestia and Panagia sections) exhibit high relative frequencies of shelf dwellers epifaunal benthic foraminifera, such as *Elphidium, Rosalina, Ammonia, Discorbis* and miliolids. These benthic foraminifera could have been reworked and transferred by turbidity currents into the deep-water depositional environment (e.g., Murray 1991, 2006).

The high P/B (over 80 %) indicates sediment deposition in the bathyal zone whereas lower values (~50 to 60 %) suggest deposition in the outer shelf zone (Murray 1991).The qualitative analysis of benthic assemblages in thesouthern HTB, and the high P/B (over 80 %, Figs. 3b, 4b, 5b) indicates that the sedimentary rocks form the Ifestia, Panagia and Kaspakas sections reflect deposition in the bathyal zone. The water depth of deposition is calculated to D=~700–1100 m. In contrast, the upper parts of the Kaminia section display P/B of ~ 50 to 60 % (Fig. 5b) and suggest sediment deposition in the outer shelf zone. The water depth of deposition is calculated to D=~200 m. This upward decrease in water depth is further indicated by the absence of deep water foraminifera, such as the benthic foraminifera *Bathysiphon* and the planktonic foraminifera *C. unicavus* and *P. nana* (e.g., Douglas & Savin 1978; Poore & Matthews 1984; Wade & Pearson 2008).

Paleoenvironmental and paleoclimate reconstruction

The late Eocene to early Oligocene time interval is characterized by significant changes in ocean circulation. Microfossils are a useful tool for paleoenvironmental/

paleoclimatic reconstruction of this interval, as planktonic foraminifera provide important information about the prevailing conditions in the water column (e.g., Kucera 2007; Ozdínová & Soták 2014) and benthic foraminifera are excellent indicators for the ocean paleoproductivity and/or the oxygenation of bottom waters (e.g., van der Zwaan et al. 1999; Jorissen et al. 2007; Ozdínová & Soták 2014). The main change in the assemblages of planktonic foraminifera associated with a significant cooling event started at the end of Eocene (e.g., Wade & Pearson 2008), which was caused by the development of glaciation in Antarctica and negatively affected the majority of planktonic foraminifera that lived in subtropical/warm surface sea waters (Molina et al. 2006).

In Lemnos Island, the deposited sediments of late Eocene to early Oligocene consist of the planktonic foraminifera *G. officinalis* and *C. cubensis*. These species are thought to live in the upper part of the water column, such as deep-water dwellers *P. nana* and *C. unicavus* (Spezzaferri 1995; Wade et al. 2000, 2007; Spezzaferri et al. 2002; Wade 2004; Pearson et al. 2006; Sexton et al. 2006). *C. unicavus* and *P. nana* are indicative of low temperature conditions (e.g., Wade et al. 2000; Pearson et al. 2001; Wade & Pearson 2008; Coccioni et al. 2009). According to benthic foraminifera of late Eocene to early Oligocene, the calcareous indicators in most cases prevail over agglutinants (~70 % calcareous, ~30 % agglutinants). Calcareous benthic foraminifera include satisfactory values of epifaunals (represented by *Cibicides/Cibicidoides, Gyroidinoides, Lenticulina*) and infaunals (represented mainly by *Bolivina, Bulimina, Globobulimina, Globocassidulina*, nodosarids). Furthermore, the BFOI index displays in most cases, values higher than 50 % identifying environments with high oxygenation in bottom waters (Kaiho 1994).

Late Eocene

During the late Eocene (outer fan, lobe facies, Ifestia section, Fig. 3), the increased P/B ratios (~84 %) indicate deposition in the bathyal zone, and it is further suggested by the high values of infaunal indicators and deep-water dwellers. *Globobulimina* is an indicator of low oxygenation in bottom waters (e.g., Sen Gupta & Machain-Castillo 1993; Triantaphyllou et al. 2009, 2016), and its high percentage (74 %, lower layers of Ifestia section, sample L65) indicates dysoxic conditions. This is also suggested by the presence of suboxic benthic foraminifera, the low values of oxic indicators and the low oxygenation index (BFOI, less than 7 %). The studied succession includes the representatives of dentoglobigerinids and turborotaliids, which were in abundance and high diversity in Mediterranean during the warm periods of Eocene (e.g., Bolli & Krasheninnikov 1977; Zivkovic & Babic 2003). However, the presence of low temperature planktonic indicators, such as paragloborotaliids, globigerinids and chiloguembelinids (e.g., Soták 2010) may indicate a gradual cooling trend since the late Eocene (e.g., Dall'Antonia et al. 2003).

Eocene/Oligocene boundary

The Eocene/Oligocene boundary is identified within the lobe facies (Ifestia section) and indicates the onset of different paleoenvironmental conditions. The oxygenation index of benthic foraminifera (BFOI) is high (73.5 %) and suggests well-oxygenated bottom waters. Additional evidence stems from the: (1) highest average of oxic indicators, (2) high values of epifaunal taxa, (3) high values of calcareous benthic foraminifera and (4) presence of suboxic indicators. The high values of the planktonic foraminifera *C. unicavus* (~ 20 %) and *P. nana* (~13 %) suggest a strong cooling event during the early Oligocene (O1 biozone) and is likely linked to the global cooling event Oi1 that has been placed at 33.55 Ma (e.g., Zachos et al. 1996; Katz et al. 2008) or at 33.65 Ma (Coxall & Wilson 2011). This event is ascribed to the expansion of the Antarctic glacers and the 405-ky eccentricity cycle of the Earth8 (4Eo–C13n cycles, Pälike et al. 2006).

Early Oligocene

The lower Oligocene deposits are represented by theseat the top of lobe facies (Ifestia section, NP21-22 biozone), the channel-fill facies (Ifestia section, NP23 biozone, bottom of NP24 biozone and Panagia section, NP24 biozone) and the shelf facies (Kaminia section, NP24 biozone). The lower Oligocene deposits at Ifestia section record accumulation in the bathyal zone (D=700–1100 m) as evidenced by the high P/B (~80%). The same conclusion can be drawn for the channel-fill deposits and comes from the results of paleobathymetry analysis, along with the high values of infaunal indicators, the values of deep-water dwellers and the presence of *Bathysiphon* as a deep-water indicator (Figs. 3, 4).

The channel-fill facies (Ifestia and Panagia section) display high relative frequencies of agglutinants, which coincide with the high values of shelf dwellers (reworking species) that were most likely transferred with turbidity currents. This hypothesis is also enhanced by the high values of *Bathysiphon* (Figs. 3a, 4a), which is common in environments with turbidity currents and is probably associated with disruption or increase of organic matter in bottom waters and subsequent dysoxic conditions (e.g., Miller 1988, 1995; Ortiz et al. 2011; Landing et al. 2012). Furthermore, some of the agglutinants were most likely redeposited, and this coexistence of in situ and reworked agglutinants is a common feature for a submarine fan system. There worked species were transferred along the slope to the deep-water environment through turbidity currents (e.g., Jones 2006; Ortiz et al. 2011). The high values of BFOI index, the increased values of oxic and suboxic indicators, the low values of dysoxic indicators and the increased presence of calcareous benthic foraminifera indicate the prevalence of high oxic conditions in the bottom waters. However, low oxygenation intervals have been identified in all sections (Ifestia section, samples L31, L65; Panagia section, samples R0.4, R7, R41; Kaminia section, samples D47, D51-54, D59). These intervals exhibit lower BFOI indexes and high values

of dysoxic indicators that are mainly composed of *Bolivina* and *Globobulimina*. These benthic foraminifera are infaunal indicators and were used to live in the upper 10 cm of sediment layers of sea bottoms with high supply of organic matter (e.g., Schmiedl et al. 2000; Jorissen et al. 2007; Thomas 2007). The high prevalence of these species may be associated with a decrease of oxygen conditions, associated to oxidation of the organic matter (e.g., Lutze & Coulbourn 1984; Corliss & Emerson 1990; Corliss 1991; Sen Gupta & Machain-Castillo 1993; Gooday 1994; Schmiedl et al. 1997; Bernhard & Sen Gupta 1999; Thomas et al. 2000; Pezelj et al. 2007; Ortiz et al. 2011). The increase of primary productivity in this time interval possibly constitutes a response to the Oi-1 cooling event as it was recorded in the Southern Ocean (Baldauf & Barron 1990; Baldauf 1992; Salamy & Zachos 1999).

The high presence of *Globobulimina* (70 %) suggests lower oxygenation during the late Eocene (Ifestia section, sample L65), while the high presence of *Bolivina* suggests similar conditions during the early Oligocene. The differences in appearance between these species, during the late Eocene to early Oligocene time interval is most likely related to different environmental conditions. *Globobulimina* is recorded in modern environments with relatively stable conditions (e.g., Rogerson et al. 2006; Koho et al. 2007; Hess & Jorissen 2009), while *Bolivina* is characterized by its opportunistic lifestyle, is common in high-energy environments and tolerant in oxygen depletion (e.g., Hess & Jorissen 2009; Ortiz et al. 2011).

C. cubensis is important planktonic foraminifera and it is employed as a high productivity indicator in the surface waters (e.g., Alegret et al. 2008). In the studied succession, high values of *C. cubensis* (over 10 %) have been recorded in the O3/O4 biozone (Rupelian; Channel-fill facies/Panagia section; shelf facies/Kaminia section). In particular, the channel-fill facies of Panagia section displays significant picks of *C. cubensis* that exceed 30 % (samples R7 and R0.2). The very common presence of planktonic foraminifera and deep-water dwellers, such as *P. nana* and *C. unicavus* that are employed for evaluating productivity in bottom waters (Ozdínová & Soták 2014) indicates high productivity along the water column. These high productivity levels could be correlated to strong mixing of waters during cold events. Such mixing could be related to a second global cooling event (Oi2) at 30–30.5 Ma, and has been identified elsewhere (e.g., Wade & Pälike 2004; Miller et al. 2008).

The shelf facies (Kaminia section, Fig. 5) display similar paleoenvironmental and paleoclimatic conditions to the lower Oligocene submarine fan deposits. They generally display well-oxygenated conditions that are interrupted by shorter intervals of well-oxygenated conditions, likely associated to the reduction of quality and quantity of organic matter (e.g., Pezelj et al. 2007). The decrease of water depth in the upper part of Kaminia section to about 200 m, along with the absence of *P. nana* and *C. unicavus* documents the shoaling a regional shoaling upwards trend, which is associated mainly to tectonic activity (Maravelis et al. 2007, 2015, 2016).

Conclusions

The new micropaleontological data collected from the upper Eocene–lower Oligocene sedimentary succession of the southern HTB provide insights to the paleoclimatological and paleoenvironmental evolution during the Eocene to Oligocene climate transition. The benthic and planktonic foraminiferal analyses, in conjunction with the P/B and paleobathymetric analysis confirm the shoaling-upward succession in Lemnos Island (from submarine fans, through slope to shallow-marine deposits) that has been already documented with sedimentological and stratigraphic criteria. The submarine fans were deposited at water depths of ~700–1100 m whereas, the overlying shelf deposits at water depths ~200 m. In the upper Eocene samples, the occurrence of the benthic foraminifera *Globobulimina* indicates dysoxic intervals in a depositional environment of generally oxic bottom-water redox conditions. The occurrence of cool planktonic representatives, such as paragloborotaliids, globigerinids and chiloguembelinids could be associated with a gradual cooling since the late Eocene. The samples from the Eocene/Oligocene boundary suggest well-oxygenated conditions of bottom waters. The abundance of *C. unicavus* certifies a significant decrease of water temperature during the early Oligocene (O1 biozone), probably linked to the global cold event Oi1. The high values of oxygen indicators in the lower Oligocene samples indicate high oxygen conditions in bottom waters. However, the common presence of *Bathysiphon* (that is associated with turbidity currents) and *Bolivina* implies decreased oxygen intervals, most likely related to high supply of organic matter. Finally, the presence of *C. cubensis*, *P. nana* and *C. unicavus* indicate increasing productivity in the water column, which is possibly correlated with the vigorous mixing of waters during cool event Oi2.

References

Agnini C., Fornaciari E., Raffi I., Catanzariti R., Pälike H., Backman J. & Rio D. 2014: Biozonation and biochronology of Paleo-

gene calcareous nannofossils from low and middle latitudes. *Newsletters on Stratigraphy* 47, 131–181. https://doi.org/10.1127/0078-0421/2014/0042

Alegret A., Molina E. & Thomas E. 2003: Benthic foraminiferal turnover across the Cretaceous/ Paleogene boundary at Agost (southeastern Spain): Paleoenvironmental inferences. *Marine Micropaleontology* 48, 251–279. https://doi.org/10.1016/S0377-8398(03)00022-7

Alegret L., Cruz L.E., Fenero R., Molina E., Ortiz S. & Thomas E. 2008: Effects of the Oligocene climatic events on the foraminiferal record from Fuente Caldera section (Spain, western Tethys). *Palaeogeography, Palaeoclimatology, Palaeoecology* 269, 94–102. https://doi.org/10.1016/j.palaeo.2008.08.006

Baldauf J.G. 1992: Middle Eocene through early Miocene diatom floral turnover. In Prothero D.R. & Berggren W.A. (Eds.): Eocene–Oligocene Climatic and Biotic Evolution. *Princeton University Press*, Princeton, 310–326.

Baldauf J.G. & Barron J.A. 1990: Evolution of biosiliceous sedimentation patterns – Eocene through Quaternary: Paleoceanographic response to polar cooling. In: Bleil U. & Thiede J. (Eds.): Geological History of the Polar Oceans: Arctic versus Antarctic. *Kluwer*, Dordrecht, 575–601.

Bandy O. 1960: General correlation of foraminiferal structure with environment. *International Geological Congress*, XXX Session (Norden) 22, 7–9.

Barbieri R. 1992: Oligocene through Palaeogene/Neogene boundary foraminifera of the northern Mesohellenic Basin (Macedonia, Greece): biostratigraphy and palaeoecologic implications. *Palaeogeography, Palaeoclimatology, Palaeoecology* 99, 193–211.

Barker P.F. & Thomas E. 2004: Origin, signature and paleoclimatic influence of the Antarctic Circumpolar Current. *Earth Science Review* 66, 143–162. https://doi.org/10.1016/j.earscirev.2003.10.003

Berger W.H. & Diester-Haass L. 1988: Paleoproductivity: the benthic/planktonic ratio in foraminifera as a productivity index. *Marine Geology* 81, 15–25.

Berggren W.A. & Prothero D.R. 1992: Eocene–Oligocene climatic and biotic evolution: An overview. In: Prothero D.R. & Berggren W.A. (Eds.): Eocene–Oligocene Climatic and Biotic Evolution. *Princeton University Press,* Princeton, 1–28.

Berggren W.A., Kent D.V. Swisher III C.C. & Aubry M.P. 1995: A revised Cenozoic geochronology and chronostratigraphy. In: Berggren W.A., Kent D.V., Swisher III C.C., Aubry M.P. & Hardenbol J. (Eds.): Geochronology, Time Scales and Global Stratigraphic Correlation. *Society for Sedimentary (SEPM)*, 212.

Bernhard J.M. & Sen Gupta B.K. 1999: Foraminifera of oxygen-depleted environments. In: Sen Gupta B.K. (Ed.): Modern Foraminifera. *Kluwer Academic Publishers*, Dordecht, 201–216.

Boll H.M. & Krasheninnikov V.A. 1977: Problems in Paleogene and Neogene correlations based on planktonic foraminifera. *Micropaleontology* 23, 436–452.

Coccioni R., Frontalini F. & Spezzaferri S. 2009: Late Eocene impact-induced climate and hydrological changes: Evidence from the Massignano global stratotype section and point (central Italy). In: Koeberl C. & Montanari A. (Eds.): The late Eocene Earth-Hothouse, Icehouse, and Impacts. *Geological Society of America Bulletin* 452, 97–118. https://doi.org/10.1130/2009.2452(07)

Corliss B.H. 1985: Microhabitats of benthic foraminifera within deep-sea sediments. *Nature* 314, 435–438.

Corliss B.H. 1991: Morphology and microhabitat preferences of benthic foraminifera from the northwest Atlantic Ocean. *Marine Micropaleontology* 17, 195–236.

Corliss B.H. & Chen C. 1988: Morphotype patterns of Norwegian Sea deep-sea benthic foraminifera and ecological implications. *Geology* 16, 716–719.

Corliss B.H. & Emerson S. 1990: Distribution of Rose Bengal stained deep-sea benthic foraminifera from the Nova Scotia continental margin and Gulf of Maine. *Deep-Sea Research* 37, 381–400.

Corliss B.H., Martinson D.G. & Keffer T. 1986: Late Quaternary deep-ocean circulation. *Geological Society of America Bulletin* 97, 1106–1121.

Coxall H. & Wilson P. 2011: Early Oligocene glaciation and productivity in the eastern equatorial Pacific; insights into global carbon cycling. *Paleoceanography* 26, 2221. https://doi.org/10.1029/2010PA002021

Coxall H.K., Wilson P.A., Pälike H., Lear C.H. & Backman J. 2005: Rapid stepwise onset of Antarctic glaciation and deeper calcite compensation in the Pacific Ocean. *Nature* 433, 53–57. https://doi.org/10.1038/nature03135

d'Atri A., Zuffa G.G., Cavazza W., Okay A.I. & Di Vincenzo G. 2012: Detrital supply from subduction/accretion complexes to the Eocene-Oligocene postcollisional southern Thrace Basin (NW Turkey and NE Greece). *Sedimentary Geology* 243–244, 117–129. https://doi.org/10.1016/j.sedgeo.2011.10.008

Dall'Antonia B., Bossio A. & Guernet C. 2003: The Eocene/Oligocene boundary and the psychrospheric event in the Tethys as recorded by deep-sea ostracods from the Massignano Global Boundary Stratotype Section and Point, Central Italy. *Marine Micropaleontology* 48, 91–106. https://doi.org/10.1016/S0377-8398(02)00163-9

den Dulk M., Reichart S., van Heyst S., Zachariasse W.J. & van der Zawan G.J. 2000: Benthic foraminifera as proxies of organic matter flux and bottom water oxygenation? A case history from the northern Arabian Sea. *Marine Micropaleontology* 161, 337–359. https://doi.org/10.1016/S0031-0182(00)00074-2

Dimitriadis S., Kondopoulou D. & Atzemoglou A. 1998: Dextral rotations and tectonomagmatic evolution of the southern Rhodope and adjacent regions (Greece). *Tectonophysics* 299, 159–173.

Douglas R.G. & Savin S.M. 1978: Oxygen isotopic evidence for the depth stratification of the Tertiary and Cretaceous planktic foraminifera. *Marine Micropaleontology* 3, 175–196.

Douglas R.G. & Woodruff F. 1981: Deep-sea Benthic Foraminifera. In: Emiliani C. (Ed.): The Sea, The Oceanic Lithosphere. *Wiley*, New York, 1233–1327.

Fenero R., Thomas E., Alegret A. & Molina E. 2012: Oligocene benthic foraminifera from the Fuente Caldera section (Spain, western Tethys): taxonomy and paleoenvironmental inferences. *Journal of Foraminiferal Research* 42, 286–304. https://doi.org/10.2113/gsjfr.42.4.286

Gibson T.G. 1988: Assemblage characteristics of modern benthic foraminifera and application to environmental interpretation of Cenozoic deposits of eastern North America. *Review of Paleobiology* 2, 777–787.

Gooday A.J. 1994: The biology of deep-sea foraminifera: a review of some advances and their applications in paleoceanography. *Palaios* 9, 14–31.

Hermelin J.O.R. & Shimmield G.B. 1995: Impact of productivity events on benthic foraminiferal faunas in the Arabian Sea over the last 150,000 years. *Paleoceanography* 10, 85–116.

Hess S. & Jorissen F.J. 2009: Distribution patterns of living benthic foraminifera from Cap Breton Canyon, Bay of Biscay: faunal response to sediment instability. *Deep-Sea Research* 56, 1555–1578. https://doi.org/10.1016/j.dsr.2009.04.003

Jorissen F.J., De Stigter H.C. & Widmark J.G.V. 1995: A conceptual model explaining benthic foraminiferal microhabitats. *Marine Micropaleontology* 26, 3–15.

Jorissen F.J., Fontanier C. & Thomas E. 2007: Paleoceanographical proxies based on deep-sea benthic foraminiferal assemblage characteristics, Volume 1 – Methods in Late Cenozoic Paleoceanography, III – Biological trancers and biomarkers, 500. https://doi.org/10.1016/S1572-5480(07)01012-3

Jones M.R. 2006: Cenozoic landscape evolution in central Queensland. *Australian Journal of Earth Sciences* 53, 433–444. https://doi.org/10.1080/08120090500499339

Kaiho K. 1994: Benthic foraminiferal dissolved-oxygen index and dissolved oxygen levels in the modern ocean. *Geology* 22, 719–722.

Kaiho K. 1999: Evolution in the test size of deep-sea benthic foraminifera during the past 120m.y. *Marine Micropaleontology* 37, 3–65.

Katz M.E., Miller K.G., Wright J.D., Wade B.S., Browning J.V., Cramer B.S. & Rosenthal Y. 2008: Stepwise transition from the Eocene greenhouse to the Oligocene icehouse. *Nature Geoscience* 1, 329–334. https://doi.org/10.1038/ngeo179

Kennett J.P. 1977: Cenozoic evolution of Antarctic glaciation, the circum-Antarctic Ocean and their impact on global paleoceanography. *Journal of Geophysical Research* 82, 3843–3860**.**

Koho K.A., Kouwenhoven T.J., DeStigter H.C. & van der Zwaan G.J. 2007: Benthic foraminifera in the Nazare´ Canyon, Portuguese continental margin: sedimentary environments and disturbance. *Marine Micropaleontology* 66, 27–51. https://doi.org/10.1016/j.marmicro.2007.07.005

Kostopoulou S., Maravelis A.G. & Zelilidis A. 2018: Biostratigraphic analysis across the Eocene-Oligocene boundary in the southern Hellenic Thrace Basin, (Lemnos Island, north Aegean Sea). *Turkish Journal of Earth Science* 27, 232–248. https://doi.org/10.3906/yer-1703-19

Kucera M. 2007: Planktonic foraminifera as tracers of past oceanic environments. *Developments in Marine Geology* 1, 213–262. https://doi.org/10.1016/S1572-5480(07)01011-1

Landing E., Patrucco-Reyes S., Andreas A.L. & Bowser S.S. 2012: First discovery of Early Palaeozoic Bathysiphon (Foraminifera)-test structure and habitat of a 'living fossil'. *Geological Magazine* 149, 1013–1022. https://doi.org/10.1017/S0016756812000155

Lawver L.A. & Gahagan L.M. 2003: Evolution of Cenozoic seaways in the circum-Antarctic region. *Palaeogeography, Palaeoclimatology, Palaeoecology* 198, 11–37. https://doi.org/10.1016/S0031-0182(03)00392-4

Lutze G.F. & Coulbourn W.T. 1984: Recent benthic foraminifera from the continental margin of northwest Africa: community structure and distribution. *Marine Micropaleontology* 8, 361–401.

Maravelis A. & Zelilidis A. 2010: Petrography and Geochemistry of the Late Eocene–Early Oligocene Submarine Fans and Shelf Deposits on Lemnos Island, NE Greece: Implications for Provenance and Tectonic Setting. *Geological Journal* 45, 412–433. https://doi.org/10.1002/gj.1183

Maravelis A. & Zelilidis A. 2011: Geometry and sequence stratigraphy of the Late Eocene–Early Oligocene shelf and basin floor to slope turbidite systems, Lemnos Island, NE Greece. *Stratigraphy and Geological Correlation* 19, 205–220. https://doi.org/10.1134/S0869593811020080

Maravelis A. & Zelilidis A. 2013: 'Unraveling the provenance of Eocene–Oligocene sandstones of the Thrace Basin, North-east Greece': discussion. *Sedimentology* 60, 860–864. https://doi.org/10.1111/j.1365-3091.2012.01369.x

Maravelis A.G., Konstantopoulos P., Pantopoulos G. & Zelilidis A. 2007: North Aegean sedimentary basin evolution during the Late Eocene to Early Oligocene based on sedimentological studies on Lemnos Island (NE Greece). *Geologica Carpathica* 58, 455–464.

Maravelis A.G., Pantopoulos G., Tserolas P. & Zelilidis A. 2015: Accretionary prism-forearc interactions as reflected in the sedimentary fill of southern Thrace Basin (Lemnos Island, NE Greece). *International Journal of Earth Sciences* 104, 1039–1060. https://doi.org/10.1007/s00531-014-1130-6

Maravelis A.G., Boutelier D., Catuneanu O., Seymour K.ST. & Zelilidis A. 2016: A review of tectonics and sedimentation in a forearc setting: Hellenic Thrace Basin, North Aegean Sea and Northern Greece. *Tectonophysics* 674, 1–19. https://doi.org/10.1016/j.tecto.2016.02.003

Miller K.G., Wright J.D. & Fairbanks R.G. 1991: Unlocking the Ice House – Oligocene–Miocene oxygen isotopes, eustasy, and margin erosion. *Journal of Geophysical Research* 96, 6829–6848. https://doi.org/10.1029/90JB02015

Miller K.G., Kominz M.A., Browning J.V., Wright J.D., Mountain G.S., Katz M.E., Sugarman P.J., Cramer B.S., Christie-Blick N. & Pekar S.F. 2005: The Phanerozoic record of global sea-level change. *Science* 312, 1293–1298. https://doi.org/10.1126/science.1116412

Miller K.G., Browning J.V., Aubry M.P., Wade B.S., Katz M.E., Kulpecz A.A. & Wright J.D. 2008: Eocene–Oligocene global climate and sea-level changes: St. Stephens Quarry, Alabama. *Geological Society of America Bulletin* 120, 34–53. https://doi.org/10.1130/B26105.1

Miller K.G., Mountain G.S., Wright J.D. & Browning J.V. 2011: A 180-million-year record of sea level and ice volume variations from continental margin and deep-sea isotopic records. *Oceanography* 24, 40–53. https://doi.org/10.5670/oceanog.2011.26

Miller W. 1988: Giant Bathysiphon (Foraminiferida) from Cretaceous turbidites, northern California. *Lethaia* 21, 363–374.

Miller W. 1995: Examples of Mesozoic and Cenozoic Bathysiphon (Foraminifera) from the Pacific Rim and the taxonomic status of *Terebellina* Ulrich, 1904. *Journal of Paleontology* 69, 624–634.

Molina E., Gonzalvo C., Ortiz S. & Cruz L.E. 2006: Foraminiferal turnover across the Eocene–Oligocene transition at Fuente Caldera, southern Spain: No cause-effect relationship between meteorite impacts and extinctions. *Marine Micropaleontology* 58, 270-286. https://doi.org/10.1016/j.marmicro.2005.11.006

Murray J.W. 1991: Ecology and paleoecology of benthic foraminifera. *John Wiley & Sons*, New York, 1–397.

Murray J.W. 2006: Ecology and Applications of Benthic Foraminifera. *Cambridge University Press*, Cambridge, 1–426.

Natland M.L. 1933: Temperature and depth ranges of some Recent and fossil foraminifera in the southern California region. *Scripps Institute of Oceanography Bulletin* 37, 1044–1066.

Nigam R. & Henriques P.J. 1992: Planktonic percentages of foraminiferal fauna in surface sediments of the Arabian Sea (Indian Ocean) and a regional model for a paleodepth determination. *Palaeogeography, Palaeoclimatology, Palaeoecology* 91, 89–98.

Nyerges A., Kocsis A.T. & Palfy J. 2020: Changes in calcareous nannoplankton assemblages around the Eocene–Oligocene climate transition in the Hungarian Palaeogene Basin (Central Paratethys). *Historical Biology*. https://doi.org/10.1080/08912963.2019.1705295

Ortiz S., Alegret L., Payros A., Orue-Etxebarria X., Apellaniz E. & Molina E. 2011: Distribution patterns of benthic foraminifera across the Ypresian–Lutetian Gorrondatxe section, Northern Spain: Response to sedimentary disturbance. *Marine Micropaleontology* 78, 1–13. https://doi.org/10.1016/j.marmicro.2010.09.004

Ozdínová S. & Soták J. 2014: Oligocene-Early Miocene planktonic microbiostratigraphy and paleoenvironments of the South Slovakian Basin (Lučenec Depression). *Geologica Carpathica* 65, 451–470. https://doi.org/10.1515/geoca-2015-0005

Ozsvárt P., Kocsis L., Nyerges A., Győri O. & Pálfy J. 2016: The Eocene-Oligocene climate transition in the Central Paratethys. *Palaeogeography, Palaeoclimatology, Palaeoecology* 459, 471–487. https://doi.org/10.1016/j.palaeo.2016.07.034

Pälike H., Norris R.D., Herrle J.O., Wilson P.A., Coxall H.K., Lear C.H., Shackleton N.J., Tripati A.K. & Wade B.S. 2006: The heartbeat of the Oligocene climate system. *Science* 314, 1894–1898. https://doi.org/10.1126/science.1133822

Pearson P.N., Ditchfield P.W., Singano J., Harcourt-Brown K., Nicholas C.J., Olsson R.K., Shackleton N.J. & Hall M.A. 2001: Warm tropical sea surface temperatures in the Late Cretaceous and Eocene epochs. *Nature* 413, 481–487. https://doi.org/10.1038/35097000

Pearson P.N., Olsson R.K., Huber B.T., Hemleben C. & Berggren W.A. 2006: Atlas of Eocene planktonic foraminifera. *Cushman Foundation for Foraminiferal Research* 41.

Pezelj D., Sremac J. & Sokac A. 2007: Palaeoecology of the Late Badenian foraminifera and ostracoda from the SW Central Paratethys (Medvednica Mt., Croatia). *Geologia Croatica* 60, 139–150. https://doi.org/10.4154/GC.2007.03

Poore R.Z. & Matthews R.K. 1984: Late Eocene-Oligocene oxygen and carbon isotope record from the South Atlantic Ocean DSDP Site 522. *Deep Sea Drilling Project Initial Reports* 73, 725–736.

Prothero D.R. 1994: The Eocene–Oligocene Transition – Paradise Lost. *Columbia University Press*, New York, 1–291.

Ring U., Glodny J., Will T. & Thomson S.N. 2010: The Hellenic subduction system: highpressuremetamorphism, exhumation, normal faulting, and large-scale extension. *Annual Review of Earth and Planetary Sciences* 38, 45–76. https://doi.org/10.1146/annurev.earth.050708.170910

Robertson A.H.F., Clift P.D., Degnan P.J. & Jones G. 1991: Paleogeographic and paleotectonic evolution of the eastern Mediterranean Neotethys. *Palaeogeography, Palaeoclimatology, Palaeoecology* 87, 289–343.

Rogerson M., Rohling E.J. & Weaver P.P.E. 2006: Promotion of meridional overturning by Mediterranean-derived salt during the last deglaciation. *Paleoceanography and Paleoclimatology* 21. https://doi.org/10.1029/2006PA001306

Salamy K.A. & Zachos J.C. 1999: Latest Eocene–Early Oligocene climate change and Southern Ocean fertility: inferences from sediment accumulation and stable isotope data. *Palaeogeography, Palaeoclimatology, Palaeoecology* 145, 61–77.

Sancay R.H. & Batı Z. 2020: Late Eocene to Early Oligocene palynostratigraphy of the Western Black Sea, Eastern Paratethys. *Turkish Journal of Earth Sciences* 29, 115–138.

Scher H. & Martin E. 2004: Circulation in the Southern Ocean during the Paleogene inferred from Neodymium isotopes. *Earth and Planetary Science Letters* 228, 391–405. https://doi.org/10.1016/j.epsl.2004.10.016

Schmiedl G., Mackensen A. & Müller P.J. 1997: Recent benthic foraminifera from the eastern South Atlantic Ocean: dependence on food supply and water masses. *Marine Micropaleontology* 32, 249–287.

Schmiedl G., Hemleben C., Keller J. & Segl M. 1998: Impact of climatic changes on the benthic foraminiferal fauna in the Ionian Sea during the last 330,000 years. *Paleoceanography* 13, 447–458.

Schmiedl G., DeBovée F., Buscail R., Charrière B., Hemleben C., Medernach L. & Picon P. 2000: Trophic control of benthic foraminiferal abundance and microhabitat in the bathyal Gulf of Lions, western Mediterranean Sea. *Marine Micropaleontology* 40, 167–188. https://doi.org/10.1016/S0377-8398(00)00038-4

Sen Gupta B.K. & Machain-Castillo M.L. 1993: Benthic foraminifera in oxygen poor habits. *Marine Micropaleontology* 20, 183–201.

Sexton P.F., Wilson P.A. & Pearson P.N. 2006: Microstructural and geochemical perspectives on planktic foraminiferal preservation: ''Glassy'' versus ''Frosty''. *Geochemistry, Geophysics, Geosystems* 7, 12–19. https://doi.org/10.1029/2006GC001291

Soták J. 2010: Paleoenvironmental changes across the Eocene–Oligocene boundary: insights from the Central-Carpathian Paleogene Basin. *Geologica Carpathica* 61, 393–418. https://doi.org/10.2478/v10096-010-0024-1

Spezzaferri S. 1995: Planktonic foraminiferal paleoclimatic implications across the Oligocene/Miocene transition in the oceanic record (Atlantic, Indian and South Pacific). *Palaeogeography, Palaeoclimatology, Palaeoecology* 114, 43–74.

Spezzaferri S., Basso D. & Coccioni R. 2002: Eocene planktonic foraminiferal response to an extraterrestrial impact at Massignano GSSP (Northeastern Appennines, Italy). *Journal of Foraminiferal Research* 32, 188–199. https://doi.org/10.2113/0320188

Thomas D.J., Lyle M., Moore JR. T.C. & Rea D.K. 2008: Paleogene deep-water mass composition of the tropical Pacific and implications for thermohaline circulation in a greenhouse world. *Geochemistry, Geophysics, Geosystems* 9. https://doi.org/10.1029/2007GC001748

Thomas E. 2007: Cenozoic mass extinctions in the deep sea: what perturbs the largest habitat on Earth. *The Geological Society of America, Special Paper* 424, 1–23. https://doi.org/10.1130/2007.2424(01)

Thomas E., Zachos J.C. & Bralower T.J. 2000: Deep-sea environments on a warm Earth: latest Paleocene-early Eocene. In: Huber B.T., MacLeod K. & Wing S.L. (Eds.): Warm Climates in Earth History. *Cambridge University Press*, Cambridge, 132–160. https://doi.org/10.1017/CBO9780511564512.006

Tranos M.D. 2009: Faulting of Lemnos Island; a mirror of faulting of the North Aegean Trough (Northern Greece). *Tectonophysics* 467, 72–88. https://doi.org/10.1016/j.tecto.2008.12.018

Tranos M.D. & Lacombe O. 2014: Late Cenozoic faulting in SW Bulgaria: fault geometry, kinematics and driving stress regimes. Implications for late orogenic processes in the Hellenic hinterland. *Journal of Geodynamics* 74, 32–55. https://doi.org/10.1016/j.jog.2013.12.001

Tranos M.D., Eleftheriadis G.E. & Kilias A.A. 2009: Philippi granitoid as a proxy for the Oligocene and Miocene crustal deformation in the Rhodope Massif (Eastern Macedonia, Greece). *Geotectonic Research* 96, 69–85. https://doi.org/10.1127/1864-5658/09/96-0069

Triantaphyllou M., Gogou A., Dimiza M., Kostopoulou S., Parinos C., Rousakis G., Geraga M., Bouloubassi I., Fleitmann D., Zervakis V., Velaoras D., Diamantopoulou A., Sampatakaki A. & Lykousis V. 2016: Holocene Climatic Optimum centennial-scale paleoceanography in the NE Aegean (Mediterranean Sea). *Geo-Marine Letters* 36, 51–66. https://doi.org/10.1007/s00367-015-0426-2

Triantaphyllou M.V., Ziveri P., Gogou A., Marino G., Lykousis V., Bouloubassi I., Emeis K.C., Kouli K., Dimiza M., Rosell-Melé A., Papanikolaou M., Katsouras G. & Nunez N. 2009: Late Glacial-Holocene climate variability at the south-eastern margin of the Aegean Sea. *Marine Geology* 266, 182–197. https://doi.org/10.1016/j.margeo.2009.08.005

van der Zwaan G.J., Jorissen F.J. & De Stigter H.C. 1990: The depth dependency of planktonic/benthic foraminiferal ratios: Constraints and applications. *Marine Geology* 95, 1–16.

van der Zwaan G.J., Duijnslec I.A.P., den Dulk M., Ernst S.R., Jannink N.T. & Kouwcrlhoven T.J. 1999: Benthic foraminifers: proxies or problems; A review of paleoecological concepts. *Earth-Science Research* 46, 213–236.

van Hinsbergen D.J.J., Hafkenscheid E., Spakman W., Meulenkamp J.E. & Wortel R. 2005: Nappe stacking resulting from subduction of oceanic and continental lithosphere below Greece. *Geology* 33, 325–328. https://doi.org/10.1130/G20878.1

Via R.K. & Thomas D.J. 2006: Evolution of Atlantic thermohaline circulation-timing of the onset of deep-water production in the North Atlantic. *Geology* 34, 441–444. https://doi.org/10.1130/G22545.1

von Quadt A., Moritz R., Peytcheva I. & Heinrich C.A. 2005: Geochronology and geodynamics of Late Cretaceous magmatism and Cu-Au mineralization in the Panagyurishte region of the Apuseni–Banat–Timok Srednogorie belt, Bulgaria. *Ore Geology Reviews* 27, 95–126. https://doi.org/10.1016/j.oregeorev.2005.07.024

Wade B.S. 2004: Planktonic foraminiferal biostratigraphy and mechanisms in the extinction of Morozovella in the late middle Eocene. *Marine Micropaleontology* 51, 23–38. https://doi.org/10.1016/j.marmicro.2003.09.001

Wade B.S. & Pälike H. 2004: Oligocene climate dynamics. *Paleoceanography and Paleoclimatology* 19, 4–19. https://doi.org/10.1029/2004PA001042

Wade B.S. & Pearson P.N. 2008: Planktonic foraminiferal turnover, diversity fluctuations and geochemical signals across the Eocene/Oligocene boundary in Tanzania. *Marine Micropaleontology* 68, 244–255. https://doi.org/10.1016/j.marmicro.2008.04.002

Wade B.S., Kroon D. & Norris R.D. 2000: Upwelling in the late middle Eocene at Blake Nose. *Geological Society of Sweden* 122, 174–175. https://doi.org/10.1080/11035890001221174

Wade B.S., Berggren W.A. & Olsson R.K. 2007: The biostratigraphy and paleobiology of Oligocene planktonic foraminifera from the equatorial Pacific Ocean (ODP Site 1218). *Marine Micropaleontology* 62, 167–179. https://doi.org/10.1016/j.marmicro.2006.08.005

Wade B.S., Pearson P.N., Berggren W.A. & Pälike H. 2011: Review and revision of Cenozoic tropical planktonic foraminiferal biostratigraphy and calibration to the Geomagnetic Polarity and Astronomical Time Scale. *Earth-Science Review* 104, 111–142. https://doi.org/10.1016/j.earscirev.2010.09.003

Wade B.S., Olsson R., Pearson P.N., Huber B.T. & Berggren W.A. 2018: Atlas of Oligocene planktonic foraminifera. *The Cushman Foundation for Foraminiferal Research, Special Publication* 46, 1–528.

Zachos J., Pagani M., Sloan L., Thomas E. & Billups K. 2001: Trends, rhythms, and aberrations in global climate 65 Ma to Present. *Science* 292, 686–693. https://doi.org/10.1126/science.1059412

Zachos J.C., Quinn T.M. & Salamy K.A. 1996: High-resolution (10^4 years) deep-sea foraminiferal stable isotope records of the Eocene-Oligocene climate transition. *Paleoceanography and Paleoclimatology* 11, 251–266.

Zivkovic S. & Babic L. 2003: Paleoceanographic implications of smaller benthic and planktonic foraminiferafrom the Eocene Pazin Basin (Coastal Dinarides, Croatia). *Facies* 49, 49–60. https://doi.org/10.1007/s10347-003-0024-z